15th CIRP Conference on Modelling of Machining Operations

# A finite element simulation for orthogonal cutting of UD-CFRP incorporating a novel fibre-matrix interface model

Alessandro Abena[a], Sein Leung Soo[a,*], Khamis Essa[a]

[a]School of Mechanical Engineering, University of Birmingham, Edgebaston, Birmingham B15 2TT, United Kingdom

* Corresponding author. Tel.: +44-121-414-4196 ; fax: +44-121-414-4201.  E-mail address: s.l.soo@bham.ac.uk

**Abstract**

The rapid increase in industrial utilisation of carbon fibre reinforced plastic (CFRP) composites in recent years has led to growing interest in numerical modelling of material behaviour and defect formation when machining CFRP. The inhomogeneous/anisotropic nature of CFRP however presents considerable challenges in accurately modelling workpiece defects such as debonding between the matrix and fibre phase following cutting operations. Much of the published literature has involved the use of zero thickness cohesive elements to represent the fibre-matrix interface, despite the inability of such elements to model compressive stresses. This paper details a new approach for characterising the interface region in a two-dimensional explicit finite element simulation when orthogonal machining unidirectional (UD) CFRP laminates. A cohesive zone model based on a traction-separation law is applied to small thickness (0.25 µm) interface elements in order to accommodate compressive failure, which is implemented via a bespoke user subroutine. Fibre fracture is based on a maximum principal stress criterion while elastic-plastic behaviour to failure is used to represent matrix damage. The influence of varying fibre orientations (45°, 90°, 135°) on predicted cutting and thrust forces were validated against published experimental data. While the former was generally within 5% of experimental data for workpieces with 90° and 135° fibre directions, predicted thrust forces were typically underestimated by ~30-60%. The corresponding chip formation mechanisms and sub-surface damage due to the different material phases were also investigated. The proposed model was able to predict composite behaviour and defect formation that was comparable to experimental high speed camera images outlined in the literature.

*Keywords:* Machining; Orthogonal cutting; Carbon fibre reinforced polymer (CFRP); Interface modelling; Cohesive behaviour.

## 1. Introduction

Fibre reinforced plastic (FRP) composite materials are increasingly being used in high performance applications within various industrial sectors, mainly due to their superior properties in terms of specific strength/stiffness, corrosion resistance, damage tolerance, resistance to fatigue as well as thermal and acoustic insulation power, when compared to conventional materials/alloys. Additionally, composite structures can generally be designed to specific loading configurations with fewer parts, leading to easier assembly of the system. Despite the ability for near net shape fabrication, machining of composite components remain necessary for removing excess material in order to meet geometrical tolerances or production of holes for joining. However in contrast to metallics, the inhomogeneous and anisotropic nature of composite material properties presents different challenges in terms of machinability. For example, common defects arising from inappropriate machining of composite parts include workpiece delamination, matrix cracking, fibre fracture/pullout, matrix burning and fibre-matrix debonding. The presence of such flaws can compromise surface integrity and lead to poor component in-service performance.

In order to minimise/eliminate workpiece damage following machining, considerable research has been carried out encompassing experimental investigations, empirical and analytical modelling together with computational/numerical simulations, in particular finite element (FE) methods. Although providing useful data and process insight, experimental led studies are generally expensive and time consuming, with considerable health and safety risks due to potential inhalation of resulting fibre debris. The primary

shortcoming of empirical models is that they are only valid within the operational window of the associated experimental trials and generally do not account for the effects of process mechanisms. Similar disadvantages are evident in analytical models, which are typically based on simplifying assumptions that do not fully capture the influence of process parameters. In contrast, computational based models allow the simulation of machining operations at varying degrees of complexity and offer the opportunity to study aspects of the process that would otherwise be difficult to evaluate experimentally (e.g. temperatures or stresses at the primary and secondary shear zones). However, the scale and accuracy of such simulations can be limited by computational cost, with predicted results requiring verification against experimental data.

A wide range of parameters must be considered when developing a FE simulation of machining composites, with the model scale having a significant influence on factors such as material behaviour and failure mechanisms [1]. In general, research to date has largely focused on modelling at either the macroscopic or microscopic length scales. The former has been extensively employed over the past 15 years, with properties of the composite workpiece usually represented in terms of an equivalent homogeneous material (EHM). The technique is applied at the macroscale where the composite material is considered as an anisotropic and homogeneous entity. Macroscopic models provide results regarding bulk chip formation but ignore interactions between the fibre and matrix, which is important to understand defect formation and propagation as well as the material behaviour during machining operations [2, 3]. The EHM approach however is relatively straightforward to implement at reasonable computational cost. Conversely, the microscopic simulation methodology is performed at the level of the different material phases (fibre, matrix, interface), each of which are modelled separately. Stress, strain and deformation in the fibre, matrix and fibre-matrix interface can be analysed. While this enables a comprehensive understanding of the cutting mechanics, such models are significantly more complex and require greater computational resources.

Generally, both approaches can be implemented simultaneously within a single model. Workpiece material near the tool can be defined according to the micro-mechanical model while the EHM procedure is used to describe material further away from the cutting zone in order to reduce computational cost of the analysis. Compared to pure EHM models, literature available detailing the hybrid approach is limited. A quasi-static simulation involving the orthogonal cutting of UD-FRP at different fibre orientations and machining parameters was developed by Rao et al. [4, 5]. Here a tool displacement boundary condition was specified, although the model was limited only to predicting failure at the first fibre via an iterative approach and therefore unable to simulate chip formation progression. Unlike quasi-static analyses, dynamic simulations can predict the failure mechanism and illustrate material behaviour during the chip formation process [6-9]. In such cases, a boundary condition based on tool velocity is typically implemented.

When employing the micromechanical modelling approach, the matrix-fibre boundary can be considered

separately, allowing the simulation and evaluation of debonding at the interface. However, in order to realise accurate predictions of workpiece subsurface damage following machining, a model capable of correctly representing the interfacial behaviour has to be utilised. Cohesive elements based on a traction-separation law are normally used to simulate very thin adhesive layers of bonded surfaces, with the majority of researchers employing a thickness value of zero [4-7]. The drawback of incorporating cohesive elements with zero thickness is that they can only be subject to tensile or shear damage and cannot undergo compressive failure, as any compressive load will generate excessive element distortion. An alternative approach where thickness of the adhesive phase is represented by a finite value allows compressive failure to be modelled. This methodology was employed by Calzada et al. [9] and demonstrated the ability of cohesive elements to operate under compressive loads, although there was no experimental validation outlined relating to the debonding mechanism.

The current paper details work on the development of a 2D FE simulation incorporating a novel fibre-matrix interface relationship for the orthogonal cutting of CFRP. A cohesive zone model based on a traction-separation law was applied to small thickness (0.25 µm) interface elements in order to accommodate compressive failure, which was implemented via a bespoke user subroutine.

## 2. Finite element model development

### 2.1. Model details

A 2D FE simulation of orthogonal cutting UD-CFRP was formulated using the commercial software ABAQUS/Explicit, with the workpiece behaviour represented by a combined micromechanical and EHM material model. The former was applied to elements near the vicinity of the tool, while the latter was defined for the remaining bulk material in order to introduce adequate stiffness in the cutting direction while reducing computational cost of the analysis. The FE model in its initial undeformed configuration together with associated boundary conditions is shown in Fig. 1.
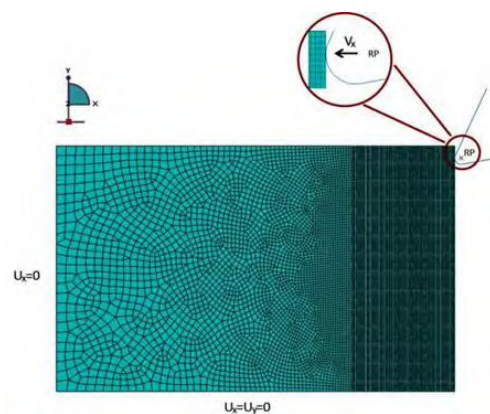


Fig. 1. Initial undeformed FE model with boundary conditions.

As the EHM section of the workpiece does not come into contact the tool, it was defined as an anisotropic homogeneous material with pure elastic behaviour. However at the cutting zone, the matrix, fibre and interface were simulated as individual phases with different constitutive response and failure models. The behaviour of the epoxy matrix is complex, being highly dependent on strain rate, temperature and loading condition. This can usually be simplified and represented by a static stress-strain curve if the cutting speed is sufficiently low. In the present work, the cutting speed ($v_c$) is fixed at 0.5 m/min, with the epoxy matrix characterised according to a static compressive stress-strain relationship at room temperature [10]. It was described as an elastic-plastic curve to failure where the plastic region is defined by the mean Von Mises yield criterion and isotropic hardening. When the Von Mises stress reaches the ultimate stress level, the element is deemed to have failed.

In contrast, carbon fibres experience brittle mode damage and hence were simulated as transversely isotropic and perfectly elastic to failure. This was described by a maximum principal stress criterion that was implemented through a user defined field (VUSDFLD) subroutine. When the maximum compressive/tensile principal stress in an element exceeds the fibre compressive/tensile strength limit, it is considered to have failed. Unlike the epoxy matrix, the carbon fibre was modelled as strain rate independent [7, 11]. The third phase relating to the matrix-fibre interface is further detailed in Section 2.2. The cutting tool was simulated as a rigid body due to its elastic modulus being considerably higher compared to the carbon fibre and epoxy matrix.

While plane strain approximation is typically utilised for simulations involving orthogonal machining of homogeneous materials, the substantial out of plane displacements when cutting composites favour the use of plane stress analysis [7]. Contact conditions were defined between each fibre and adjacent matrix phases as well as between two consecutive fibres, which were activated using the contact penalty algorithm. Frictional properties of the workpiece material were represented by the Coulomb model where the friction coefficient varied depending on the fibre orientation, i.e. 0.6, 0.8 and 0.6 for fibre directions of 45°, 90° and 135° respectively. A tie constraint was defined to initially bond all of the individual phases. The workpiece mesh comprised four node plane stress elements with reduced integration (CPS4R) for the matrix, fibre and EHM phases, while COH2D4 cohesive elements were employed for the matrix-fibre interface sections. In addition, triangular elements were utilised in the EHM region for mesh transition. The element size in the micromechanical zone was 1 μm while for the EHM area, element dimensions increased with distance from the cutting zone. The cutting parameters and composite fibre orientations used in the simulations are detailed in Table 1.

Table 1. Machining parameters and material fibre orientations.

| Tool geometry | 5 μm cutting edge radius, 10° clearance angle, 25° rake angle |
|---|---|
| Cutting speed | 500 mm/min |
| Depth of cut | 15 μm |
| Fibre orientations | 45°, 90°, 135° |

## 2.2. Cohesive zone modelling

The interface region between the matrix and fibre can be modelled as a discrete phase incorporating separate constitutive relationship and damage criteria. Failure of the interface elements can therefore be used to represent debonding between the matrix and fibre phases in composite materials subject to machining operations. The two principal techniques for introducing interface/adhesive phases in a numerical model are either by implementing a continuum description of the material or defining a traction-separation law within the cohesive element [12]. The first approach is normally employed when the thickness of the adhesive phase is finite and can be characterised by conventional material/damage models. Here, element failure under tension, compression and shear conditions can be simulated.

Conversely, when the adhesive phase thickness is negligibly small (typically near or equal to zero), micromechanical based models incorporating zero thickness cohesive elements are generally applied, such as for the matrix-fibre interface in CFRP composite materials. However, the conventional traction-separation law inherent within cohesive elements only accommodates failure under tension and shear behaviour. For the present work, a novel cohesive zone model based on extending the traction-separation law of the cohesive elements to include response and damage under compression was developed. This was achieved by introducing a small thickness (0.25 μm) for each cohesive element (to allow thinning due to loading) and its behaviour incorporated into the FE model via a bespoke user material subroutine (VUMAT).

For a two-dimensional model, the cohesive elements possess two components of separation, which act normal and parallel to the element. In the former, the mechanical response due to compression and tension effects (as a function of displacement) varied according to the distribution illustrated in Fig. 2.
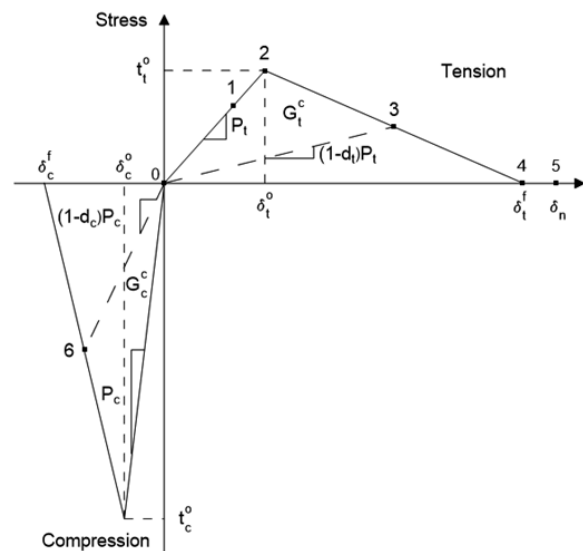


Fig. 2. Mechanical constitutive response of cohesive elements under tensile and compressive loads implemented via VUMAT subroutine.

In contrast, shear stress variation with respect to displacement in the cohesive elements (acting in the parallel direction) was equivalent for both positive and negative values as shown in Fig. 3. The stress response of the cohesive elements/interface region detailed in Figs. 2 and 3 are functions of three principal parameters, which are:

- Penalty stiffness ($P_{n/s}$)
- Stress or displacement at the damage initiation ($t^o_{n/s}, \delta^o_{n/s}$)
- Fracture energy ($G^C_{n/s}$)

Regardless of the loading condition, the mechanical stress constitutive response can be divided into three distinct regions taking into account the elastic behaviour and material strength degradation to failure as described in Eq. 1:

$$t_{n/s} = \begin{cases} P\delta_{n/s} & \Leftarrow & \delta^{max}_{n/s} \leq \delta^o_{n/s} \\ (1-d_{n/s})P\delta_{n/s} & \Leftarrow \delta^o_{n/s} < \delta^{max}_{n/s} < \delta^f_{n/s} \\ 0 & \Leftarrow & \delta^{max}_{n/s} \geq \delta^f_{n/s} \end{cases} \quad (1)$$
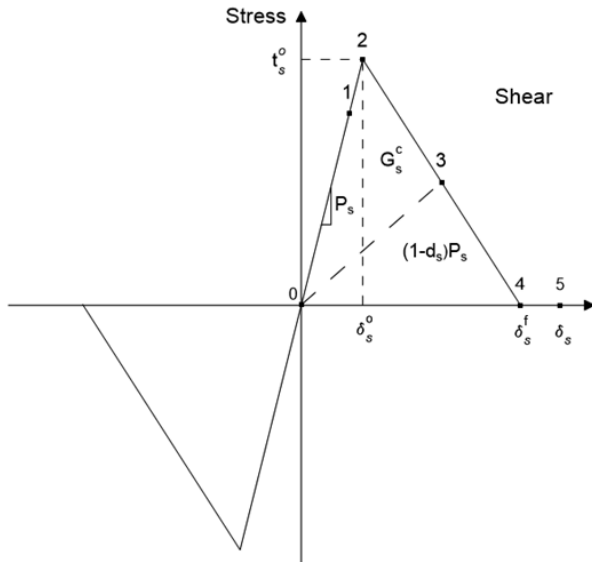


Fig. 3. Mechanical constitutive response of cohesive elements under shear loads implemented via VUMAT subroutine.

The fracture energy represents the area below the stress-displacement curve between the origin and failure point ($\delta^f$). Corresponding strains, ε (tensile, compressive and shear) are related to displacement by means of Eq. 2 and Eq. 3, where the constitutive thickness $T_o$ is assumed to be unity, while t and c indicates tensile and compressive behaviour respectively.

$$\varepsilon_n = \frac{\delta_n}{T_o}, \quad n = t, c \quad (2)$$

$$\varepsilon_s = \frac{\delta_s}{T_o} \quad (3)$$

The mechanical constitutive response is initially composed of linear elastic behaviour (point 1 in both Fig. 2 and Fig. 3) up to the moment of damage initiation (point 2), which is described in Eq. 4:

$$\overline{t} = \begin{Bmatrix} t_n \\ t_s \end{Bmatrix} = \begin{bmatrix} P_n & 0 \\ 0 & P_s \end{bmatrix} \begin{Bmatrix} \varepsilon_n \\ \varepsilon_s \end{Bmatrix} = \overline{\overline{P}}\overline{\varepsilon}, \quad n = t, c \quad (4)$$

where $\overline{t}$, $\overline{\overline{P}}$ and $\overline{\varepsilon}$ represent the stress vector, stiffness matrix and strain vector respectively. At the onset of workpiece damage, degradation of the adhesive phase is represented by a reduction of its stiffness property (point 3) according to relationship in Eq. 5.

$$P^d_{n/s} = P_{n/s}(1-d_{n/s}), \quad n = t, c \quad (5)$$

A scalar damage variable $d_{n/s}$ is introduced for each mode of failure by considering a linear damage evolution based on the formula by Camanho and Davila [13], which is expressed by Eq. 6:

$$d_{n/s} = \frac{\delta^f_{n/s}(\delta^{max}_{n/s} - \delta^o_{n/s})}{\delta^{max}_{n/s}(\delta^f_{n/s} - \delta^o_{n/s})}, \quad d_{n/s} \in [0,1]; \quad n = t, c \quad (6)$$

where $\delta^o_{n/s}$, $\delta^f_{n/s}$ and $\delta^{max}_{n/s}$ represent the displacement at damage initiation, displacement at failure and maximum displacement over the analysis duration respectively. However the tensile, compression and shear stress responses were uncoupled and considered separately. The segments 03 and 06 detailed in Fig. 2 as well as 03 in Fig. 3 represent the unloading stage of the cohesive elements following the inception of damage. Once displacement reaches the critical failure value, the element is deleted.

## 3. Results and discussion

Fig. 4 shows the predicted cutting forces from the current FE simulation incorporating the novel cohesive zone relationship compared against corresponding experimental and numerical FE results reported by Calzada et al. [9]. The experimental data revealed a reduction in cutting forces with increasing fibre orientation from 45° to 135°. The predicted cutting forces obtained from both the present simulation and numerical FE results in the literature [9] showed equivalent trends and exhibited close agreement to the experimental values for fibre angles of 90° and 135°, but were underestimated for those oriented at 45°. In contrast, the trend in predicted thrust force using the new cohesive zone model showed a minimum for the 90° oriented CFRP workpiece, which contradicted both the experimental and numerical data outlined by Calzada et al. [9] where forces decreased with larger fibre orientations, see Fig. 5. However, thrust forces were under predicted by up to ~ 60% in both FE models when cutting workpieces with 45° and 90° fibre directions. This was

most likely attributed to the failure and subsequent deletion of elements during the analysis along the cutting path, thereby causing a relaxation in the force component due to the loss of contact between the tool and workpiece.
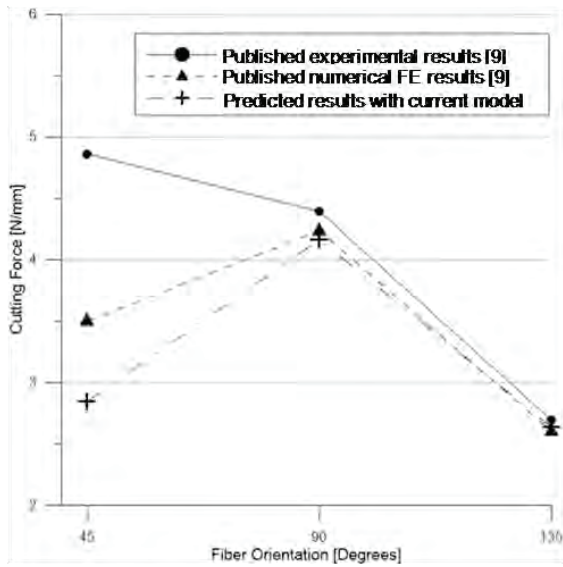


Fig. 4. Comparison between experimental and predicted cutting forces at different fibre orientations (45°, 90°, 135°).
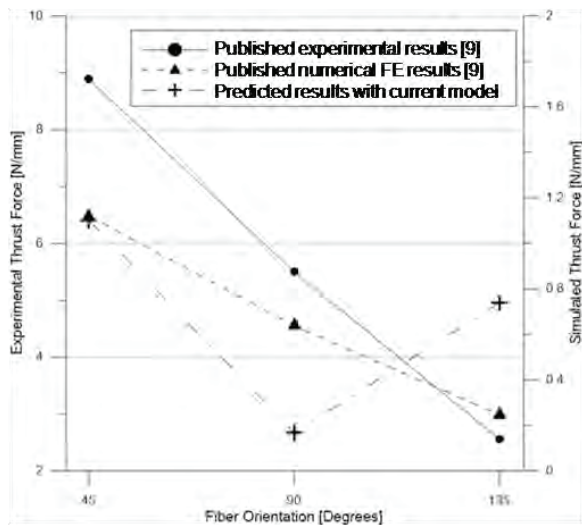


Fig. 5. Comparison between experimental and predicted thrust forces at different fibre orientations (45°, 90°, 135°).

Fig. 6 shows the predicted failure modes observed for the different CFRP fibre orientations following orthogonal machining. For the 45° fibre orientation shown in Fig. 6(a), the failure mode comprised only a single fracture situated ahead of the tool, with damage principally caused by shearing rather than bending stresses. Subsurface damage in terms of debonding and matrix failure was also evident. Conversely, fibres in the 90° direction were subject to multi-fracture damage, which occurred primarily in two different locations, see Fig. 6(b). The first fracture occurred at approximately the

depth of cut region, which initiated at the point of contact between the tool and workpiece. As machining progressed, the fracture continued to propagate through successive fibres ahead of the tool along the cutting plane. The second crack commenced below the cutting path due to bending stresses from the cutting operation. Here, damage propagated towards the cutting plane along the fibres. As the matrix represents a weaker phase of the material, failure was primarily due to compressive stresses from the surrounding fibres.

With regard to the 135° fibre orientation detailed in Fig. 6(c), the first fibre was seen to undergo damage ahead of the tool above the cutting plane. As cutting progresses, sections of the first and second fibre come into contact as the matrix layer between them fails. The second fibre starts to deform under bending followed by the matrix phase within the subsurface, causing separation between the matrix and first fibre leading to substantial damage beneath the cutting plane. The predicted damage modes in each of the different fibre orientations were largely similar to corresponding experimental high speed video imagery reported by Calzada et al. [9].
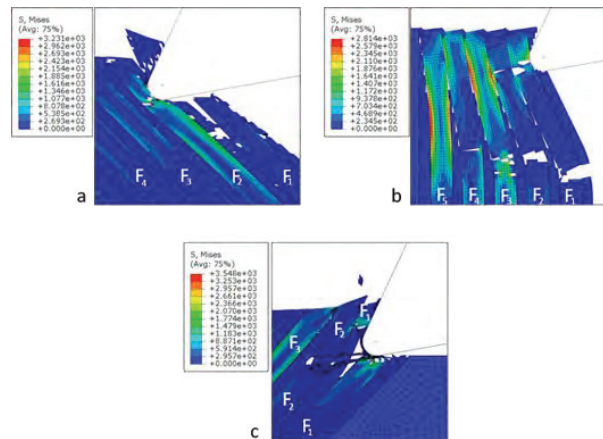


Fig. 6. Failure mode for (a) 45°, (b) 90° and (c) 135° fibre orientations.

Fig. 7 shows the simulated debonding damage using the new interface model when machining the 90° oriented fibres. Cohesive element deletion was primarily triggered by compressive loading at the interface during cutting. The tool pushed the fibre towards the matrix leading to a compressive force, which acts on the interfacial elements, as shown in Fig. 7. The result demonstrates that an interfacial model considering only tensile and shear behaviour is not sufficient to accurately simulate workpiece subsurface damage.
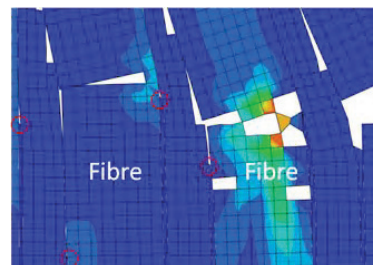


Fig. 7. Debonding simulation for 90° fibre orientation.

## 4. Conclusions

A 2D finite element model incorporating a new matrix-fibre interface damage constitutive relationship that allows cohesive elements to fail under compression as well as tension and shear was developed to simulate orthogonal cutting of UD-CFRP composite material. Different fibre orientations were considered with the model validated in terms of cutting and thrust forces as well as chip formation mechanisms against published experimental and numerical data. While the predicted cutting forces showed close agreement with experimental results, the thrust forces were generally underestimated. Furthermore, the simulated failure modes and chip formation mechanisms generally agree with reported experimental high speed camera images involving orthogonal cutting of CFRP in the literature. The results indicate that compressive failure at the interface must be considered in numerical models in order to achieve accurate subsurface damage prediction. Future work to develop the model will involve in-depth experimental trials (performed in-house) to analyse the debonding mechanism between the fibre and matrix phases in order to improve the damage criterion and better simulate workpiece defects following machining. This will also enable validation of the cohesive zone model. Mesh size sensitivity analysis to assess its effects on machining behaviour will also be carried out. Additionally, CFRP composites with different fibre orientations will be evaluated to further verify the model.

## References

[1] Dandekar CR, Shin YC. Modeling of machining of composite materials: A review. Int J Mach Tool Manuf 2012; 57:102-121.

[2] Santiuste C, Soldani X, Miguélez MH. Machining FEM model of long fiber composites for aeronautical components. Compos Struct 2010; 92:691-698.

[3] Cantero JL, Santiuste C, Marín N, Soldani X, Miguélez H. 2D and 3D approaches to simulation of metal and composite cutting. In: AIP Conference Preoceedings. AIP Publishing; 2012. p. 651:659-1431.

[4] Rao GVG, Mahajan P, Bhatnagar N. Micro-mechanical modeling of machining of FRP composites – Cutting force analysis. Compos Sci Technol 2007; 67:579-593.

[5] Rao GVG, Mahajan P, Bhatnagar N. Machining of UD-CFRP composites: Experiments and finite element modeling. In: Proceedings of the 13th European Conference on Composite Materials (ECCM13); 2-5 June 2008, Stockholm, Sweden, CD.

[6] Rao GVG, Mahajan P, Bhatnagar N. Machining of UD-GFRP composites chip formation mechanism. Compos Sci Technol 2007; 67:2271-2281.

[7] Dandekar CR, Shin YC. Multiphase Finite element modeling of machining unidirectional composites: Prediction of debonding and fiber damage. J Manuf Sci Eng-Trans ASME 2008; 130:1-12.

[8] Chennakesavelu, G. Orthogonal machining of uni-directional carbon fiber reinforced polymer composites. Bachelor Thesis in Engineering. Golden Valley Institute of Technology 2006.

[9] Calzada KA, Kapoor SG, DeVor RE, Samuel J, Srivastava AK. Modeling and interpretation of fiber orientation-based failure mechanisms in machining of carbon fiber-reinforced composites. J Manuf Proces 2012; 14:141-149.

[10] Littell JD, Ruggeri CR, Goldberg RK, Roberts GD, Arnold WA, Binienda WK. Measurement of epoxy resin tension, compression and shear stress-strain curves over a wide range of strain rates using small test specimens. J Aerospace Eng 2008; 21:162-173.

[11] Zhou Y, Wang Y, Jeelani S, Xia Y. Experimental study on tensile behaviour of carbon fiber and carbon fiber reinforced aluminium at different strain rate. Appl Compos Mater 2007; 14:17-31.

[12] ABAQUS User's Manual, version 6.13.

[13] Camanho PP, Davila CS. Mixed-mode dechoesion finite elements for the simulation of delamination in composite materials. NASA/TM-2002–211737 2002; 1:37.